Research Article

Synergistic effect of carbon nanotubes, copper and silver nanoparticles as an efficient electrochemical sensor for the trace recognition of amlodipine besylate drug

Gowhar A. Naikoo[1] · Umar J. Pandit[2] · Mehraj U. D. Sheikh[2] · Israr Ul Hassan[3] · Gulzar A. Khan[2] · Ajmal R. Bhat[4] · Ratnesh Das[2] · Ridha Horchani[5]

Received: 6 March 2020 / Accepted: 22 April 2020 / Published online: 28 April 2020

Abstract
The electrochemically functionalized multiwalled carbon nanotubes/copper nanoparticles (*f*MWCNT/CuNPs) carbon paste electrode (*f*MWCNT/CuNPs-CPE) was successfully modified by silver nanoparticles (AgNPs) via electrocatalytic process. The formation of modified electrode (AgNPs/**f**MWCNT/Cu NP-CPE) was observed by Field Emission Scanning Electron Microscopy and X-ray diffraction techniques. The as-prepared electrodes were explored for the trace recognition of calcium channel blocker drug amlodipine besylate (ADB) using cyclic voltammetry and electrochemical impedance spectroscopy measurements. Kinetic parameters like electron transfer coefficient (α), charge due to adsorption (Q_{ads}), surface coverage (Γ), charge transfer coefficient (R_{ct}), and apparent electron-transfer rate constant (k_{app}) for the designed electrodes were evaluated. The nanoparticles based electrochemical sensor displayed high sensitivity, good selectivity and favorable catalytic ability for the oxidation of amlodipine besylate. The fabricated electrodes showed good reproducibility and stability towards the determination of anti-hypertensive drug ADB.

Keywords Electrochemical sensor · Functionalized carbon nanotubes · Amlodipine besylate

Abbreviations

Ag NPs	Silver nanoparticles
*f*MWCNT/Cu NPs	Functionalized multiwalled carbon nanotubes/copper nanoparticles
CPE	Carbon paste electrode
CV	Cyclic voltammetry
MWCNTs	Multiwalled carbon nanotubes
ADB	Amlodipine besylate
BR	Britton-Robinson
FESEM	Field Emission Scanning Electron Microscope
SWAdV	Square wave adsorptive stripping voltammetry
EIS	Electrochemical impedance spectroscopy
AdSWV	Adsorptive square wave voltammetry
LOD	Limit of detection
LOQ	Limit of quantification

1 Introduction

The development of highly efficient electrochemical sensors using nanostructures of metal and metal oxides has attracted the researchers for the qualitative and quantitative analysis of organic molecules including pharmaceutical drugs and related molecules in biological and

✉ Gowhar A. Naikoo, gahmed@du.edu.om; naikgowhar@gmail.com; Umar J. Pandit, umarche@gmail.com | [1]Department of Mathematics and Sciences, College of Arts and Applied Sciences, Dhofar University, Salalah, Sultanate of Oman. [2]Department of Chemistry, Dr. Harisingh Gour University, Sagar, M.P., India. [3]College of Engineering, Dhofar University, Salalah, Sultanate of Oman. [4]Department of Chemistry, Govt; Degree College, Bijbehara, Jammu and Kashmir, India. [5]College of Science, Sultan Qaboos University, Muscat, Sultanate of Oman.

environmental concern [1]. In addition researchers have explored conducting polymers with metal and metal oxide nanoparticles and carbon nanotubes to enhance the sensitivity, stability and reproducibility of electrochemical sensors [2]. Indeed, the employment of gold (Au) and platinum (pt) based electrochemical sensors have shown incredible results. However, there application on commercial bases is restricted due to the limited reserves and high costs associated with them [2]. So, the selectivity of effective electrode modifiers has become a big challenge for the modern surface science technology [1]. To overcome the these issues, researchers have successfully explored alternative options such as ca-doped ZnO materials [1], nanosilica modified sensors [2], amberlite XAD-4 modified electrodes [3], Ruthenium doped TiO2/reduced graphene oxide [4], nanoclay-based electrochemical sensors [5], coreshell nanostructure modified electrodes [6], maghemite nanocrystals decorated multi-wall carbon nanotubes [7], ZnO/G nano composite modified carbon paste electrodes [8], silver doped TiO_2/CNTs [9], Pt-Ni bimetallic nanoparticles [10] and platinum-cobalt and platinum-nickel bimetallic nanoparticles [11] for the qualitative and quantitative analysis of antihistamine, anti- inflammatory drugs along with for the biological and environmental matters.

Designing an electrochemical sensor for the promising potential applications is a debonair task however, the vital issues to take into consideration for fabricating such sensors includes minimal cost, low toxicity, easy renewable surface and the potential for real time monitoring [12, 13]. Herein, we attempt to design, fabricate and characterize *f*MWCNT/CuNP-CPE decorated with AgNPs. As Ag and Cu are non-toxic, readily available and possess appreciable electrochemical and photocatalytic properties [14]. Nanoparticles supported on MWCNTs provide extra roughness to the conductive sensing interface and improved the electrocatalytic performance and conductive properties [15, 16]. The designed electrode was further subjected to investigate an anti-hypertensive ADB drug. ADB has the highest oral bioavailability and longest half-life of elimination among several dihydropyridine derivatives [17]. Several analytical procedures have been reported for the determination of ADB in blood plasma and pharmaceutical preparations [18–22].

2 Experimental

2.1 Chemicals and reagents

Multiwalled carbon nanotubes (MWCNT) with outer diameter 5–20 nm, inner diameter of 2–10 nm, tube length of about 5–20 µm and purity > 95 wt%, $Cu(NO_3)_2{\cdot}3H_2O$, $AgNO_3$ and ADB (purity ≥ 98%) were purchased from Sigma, India. All other chemicals and reagents were used of analytical grade (Merck, India). All solutions and reagents were prepared in doubly distilled water. A stock solution of ADB 4 mM was prepared by dissolving 0.142 mg ADB in 10 mL ethanol. Standard solutions of ADB were prepared by diluting appropriate volumes of stock solution with ethanol and supporting electrolyte. A 0.05 M Britton-Robinson (BR) buffer with *p*H 5.6–12.0 was used as supporting electrolyte. The *p*H adjustments were carried out by 0.01 M NaOH.

2.2 Instrumentation

A NOVA software controllable Metrohm Autolab B.V. PGSTAT128N electrochemical workstation equipped with a three electrode assembly was employed for electrodeposition and electrochemical measurements. Systronics µpH 361 Digital Analyzer was used for maintaining the pH of all solutions. Frontline sonicater and Remi 8C Laboratory Centrifuge were used for the preparation of fMWCNT/Cu nanohybrids and to affect complete dissolution of solutions. The morphological characterization of modified electrode surfaces was performed by using NOVA NANOSEM 450 FESEM and Bruker D-8 X-ray diffractometer using Cu-Kα radiations.

2.3 Fabrication of electrochemical sensor

2.3.1 Synthesis of functionalized MWCNT/Cu hybrids

The chemical functionalization of MWCNTs were carried out by dissolving in the mixture of concentrated H_2SO_4 and HNO_3 (3:1, v/v), and sonicating it for 5 h. The oxidative acid treatment of MWCNTs using acid mixture such as H_2SO_4/HNO_3 [23–27] is used for the successful functionalization of –COOH on the opening end of the MWCNTs. During the treatment, a strong interaction between the oxidizing acid molecules and CNTs results in creation of defect sites on the graphite lattice. Consequently, these defect sites involves the replacement of one carbon atom from the CNT lattice with one or two more oxygen's to form functional groups such as carboxylic acid (–COOH) on the CNT surface [28] and results in the functionalization of –COOH on the opening end of the CNTs. The resulting *f*MWCNTs were separated by centrifugation at 8000 rpm and washed with double distilled water till pH of MWCNTs became neutral, finally dried in oven at 120 °C. 10 mg of these functionalized MWCNTs were dispersed in an ultrasonic bath for about 8 min and then stirred on a magnetic stirrer with drop wise addition of 0.01 M $Cu(NO_3)_2$ solution at room temperature. The stirring was continued for 20 h followed by separation of solid *f*MWCNT/Cu nanohybrids

by centrifugation at 5000 rpm. The solid product was dried under IR lamp to completely evaporate the solvent [29].

2.3.2 Preparation of *f*MWCNT/Cu hybrid carbon paste electrode

21.5 mg paraffin oil, 8.5 mg *f*MWCNT/Cu hybrid and 10.5 mg carbon powder was taken and manually homogenized to form a paste. The paste was filled in 2 mm polyethylene syringes pre-inserted Cu wire for external electric contact. Smoothening of electrode surface was accomplished by mechanically pressing the paste from the top and rubbing against a smooth and clean weighing paper. The electrode was designed as *f*MWCNT/Cu NP-CPE. Bare carbon paste electrode was prepared by mixing 13.6 mg paraffin oil and 6.4 mg carbon powder and similar procedure was followed for its fabrication and regeneration of smoothed surface. The fabricated electrodes were electrochemically activated by applying ten cyclic potential sweeps from -1.0×10^3 mV to $+2.0\ 10^3$ mV in 0.1 M nitric acid solution at the scan rate of 50 mVs^{-1}.

2.3.3 Electrode surface modifications with silver nanoparticles

The electrodeposition of nanoparticle film over the surface of electrode is an electrocatalytic process and the growth, purity, shape and thickness of nanofilm over electrode surface depends on concentration of analyte, number of cyclic sweeps and scan rate. The surface of fabricated *f*MWCNT/Cu NP-CPE was modified with Ag NPs by potentiodynamic deposition of Ag NPs. The effect of Ag NPs deposition was analyzed for test solution. The best peak response in terms of peak current intensities was observed with scan rate of 25mVs^{-1} for 15 cycles in the potential range of -1.0×10^3 mV to $+1.0\times10^3$ mV. The electrode was immersed in a solution of 10 mM $AgNO_3$ containing 10 mM KNO_3. The solution was stirred for 10 min at room temperature, eventually, Ag NPs film was developed over the electrode surface by performing 15 consecutive cyclic potential sweeps at a scan rate of 25 mVs^{-1} in the given potential range. This electrode was designed as Ag NP/*f*MWCNT/Cu NP-CPE and thoroughly washed with distilled water and dried at room temperature. For comparison of studies Ag NP/*f*MWCNT-CPE was also fabricated via same procedure. The description of electrode surface modification with silver nanoparticles (Ag NPs) is shown in Scheme 1.

2.4 Pharmaceutical sample preparation

In all voltammetric studies exactly ten locally purchased Amlodac 5 and Amlopin tablets (containing 5 mg Amlodipine) were manually grounded to homogenized powder in a mortar pestle. An accurately weighed (0.071 mg of this powder was dissolved in appropriate volume of solvent and supporting electrolyte to prepare stock solutions of pharmaceutical sample. The solution was sonicated for 20 min to affect complete dissolution and stored for further assay. Working solutions were prepared by transferring suitable aliquots of the stock solution and diluting with BR buffer and supporting electrolyte.

2.5 Blood and urine sample

Human blood (for serum and plasma sample preparation) and urine samples were collected from a healthy volunteer after obtaining there formal consents. The blood samples were centrifuged at 5000 rpm for 30 min at room temperature to separate serum and plasma within 1 h of collection and kept frozen until analysis. The separated biological samples were deproteinized by adding 2 mL of acetonitrile. After vortexing for 30 s, samples were centrifuged at 5000 rpm for 15 min to eliminate protein residues. The supernatant was decanted and diluted with BR buffer (pH 10.2).

2.6 Voltammetric procedures

The required volume of the stock solution of standard and pharmaceutical sample of ADB was placed in a 50 mL beaker. The total volume was made to 25 mL with appropriate quantities of BR buffer (pH 10.2) and solvent. Square wave adsorptive stripping voltammetry (SWAdV) was employed for determining ADB. The optimized parameters

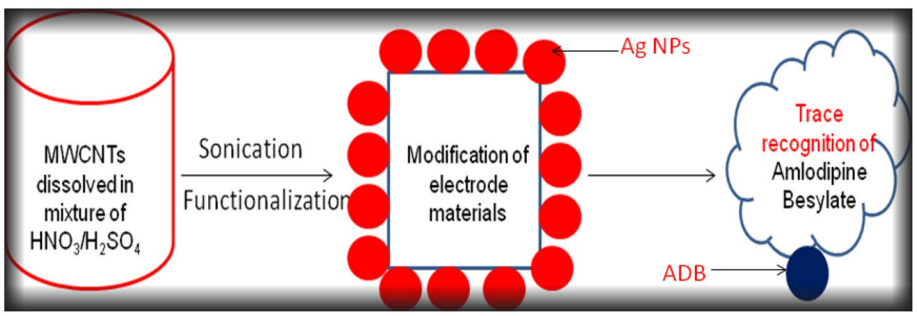

Scheme 1 Electrode surface modification with silver nanoparticles (Ag NPs)

were: accumulation potential: 5.0 mV, accumulation time: 90 s, equilibrium time: 10 s, square wave frequency: 50 Hz, step potential: 5 mV, modulation amplitude: 50 mV. Voltammograms were recorded in anodic direction from 0.0 mV to $+8.0\times10^2$ mV. EIS study was performed at open circuit potential in the frequency range 10^{-1}–10^6 Hz.

3 Results

3.1 Spectral and morphological characterization

X-ray diffraction analysis of MWCNT, *f*MWCNT/Cu hybrid and Ag NP-*f*MWCNT/Cu indicate the formation of nanoparticles film on *f*MWCNT-CPE surface (Fig. 1). The analysis was carried out in diffraction angle ranging from 2θ = 10°–90°, using Cu-Kα radiation (λ = 1.5401 Å). The XRD patterns of *f*MWCNT shows the diffusive diffraction peaks appearing as small noises at 2θ values of 29.15°, 44.80° and 52.25° corresponding to *d*-spacing and lattice planes of 3.06 Å [002], 2.02 Å [111] and 1.75 Å [200] respectively [30]. After formation of *f*MWCNT/ Cu hybrid, the XRD patterns obtained with diffraction peak at 2θ values of 28.51°, 35.0°, 43.03°, 62.01°, 72.51° and 77.88° indexed to *d*-spacing and lattice planes at 3.12 Å [110], 2.56 Å [111], 2.08 Å [200], 1.48 Å [220], 1.30 Å [311] and 1.22 Å [222] respectively. However, the electrodeposition of Ag NPs film on *f*MWCNT/ Cu hybrid, the diffractions pattern of both Cu and Ag are distinctly observed (JCPDS file no. 04.783). The presence of these peaks confirmed occurrence of metallic Cu and Ag on the surface of *f*MWCNT.

The morphological and topographical visualization of surface of *f*MWCNT-CPE, *f*MWCNT/Cu NP-CPE, AgNP-*f*MWCNT-CPE and Ag NP/*f*MWCNT/Cu NP-CPE were performed by FESEM and has given a solid confirmation of presence of Cu and Ag NPs on the surface of MWCNTs. The FESEM monograph of *f*MWCNT-CPE shown in Fig. 2a clearly shows dispersion of *f*MWCNTs over the surface of carbon paste. The *f*MWCNTs are homogenously spread without agglomeration and looking twisted, bent and tangled. The formation of *f*MWCNT/Cu hybrid was clearly observed in FESEM monographs (Fig. 2b) while the electrodeposition of Ag NPs over *f*MWCNTs is visible in Fig. 2c. However, after the electrodeposition of Ag NPs over *f*MWCNT/Cu hybrid surface agglomerates which are almost regular and homogeneously dispersed over the surface (Fig. 2d**)**.

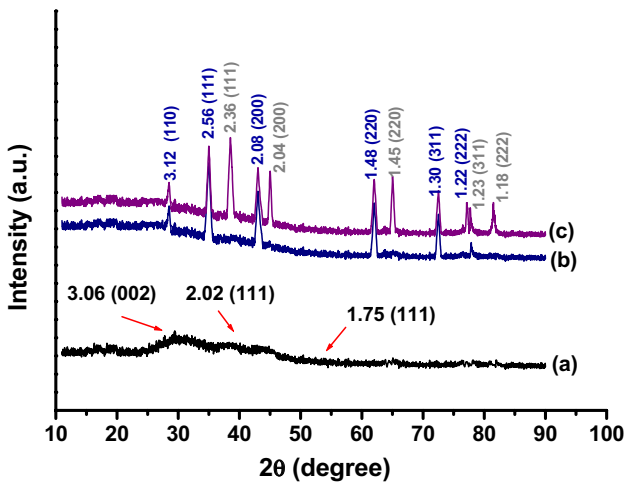

Fig. 1 XRD patterns of (a) MWCNTs, (b) MWCNT/Cu NPs and (c) Ag NP/MWCNT/Cu NPs

3.2 Cyclic voltammetric characterization of electrode

The surface feature of bare and modified CPEs were characterized by CV employing 1.0 mM $K_3Fe(CN)_6$ probe in 0.1 M KCl solution. The quasi-reversible one electron redox behavior of $Fe(CN)_6^{3-/4-}$ ions were observed on the bare CPE with ΔE_p (anodic and cathodic peak separation) of 3.62×10^2 mV at scan rate of 50 mVs^{-1}. However, after the modification of CPE with *f*MWCNT, Cu NPs and Ag NPs, a decrease in ΔE_p was observed with increase in peak current. The surface areas of the electrodes were obtained by performing cyclic voltammetric measurements of the probe at different scan rates and employing Randles–Sevick equation [31]:

$$I_{pa} = 0.4463\left(\frac{F^3}{RT}\right)^{1/2} n^{3/2}A_0D_0^{1/2}Cv^{1/2} \quad (1)$$

where I_{pa} is anodic peak current, n is the number of electrons transferred, A_0 is surface area of the electrode (cm^2), D_0 is diffusion coefficient, C is concentration of $Fe(CN)_6^{3-/4-}$ and υ is the scan rate, R is molar gas constant (8.314 JK^{-1} mol^{-1}) and F is Faraday's constant (96,480 C mol^{-1}). For 1.0 mM $K_3Fe(CN)_6$ in 0.1 M KCl at T = 298 K, n = 1 and $D_0 = 7.6\times10^{-6}$ cm^2s^{-1}. The surface area is calculated from the slope obtained from plot of I_{pa} versus $\upsilon^{1/2}$. In the present work, the surface area of the b-CPE was calculated to be 0.052 cm^2 and the microscopic surface area for *f*MWCNT-CPE, *f*MWCNT/Cu NP-CPE, Ag NP/*f*MWCNT-CPE and AgNP/*f*MWCNT/Cu NP-CPE was found as 0.272 cm^2, 0.521 cm^2, 0.636 cm^2 and 0.965 cm^2 respectively.

3.3 Electrochemical impedance spectroscopic (EIS) characterization of electrode

EIS is performed to investigate the surface characteristics surface modified electrode material as an ultra-capacitor and to elucidate the differences among the electrochemical performance of bare and modified CPEs. The Nyquist

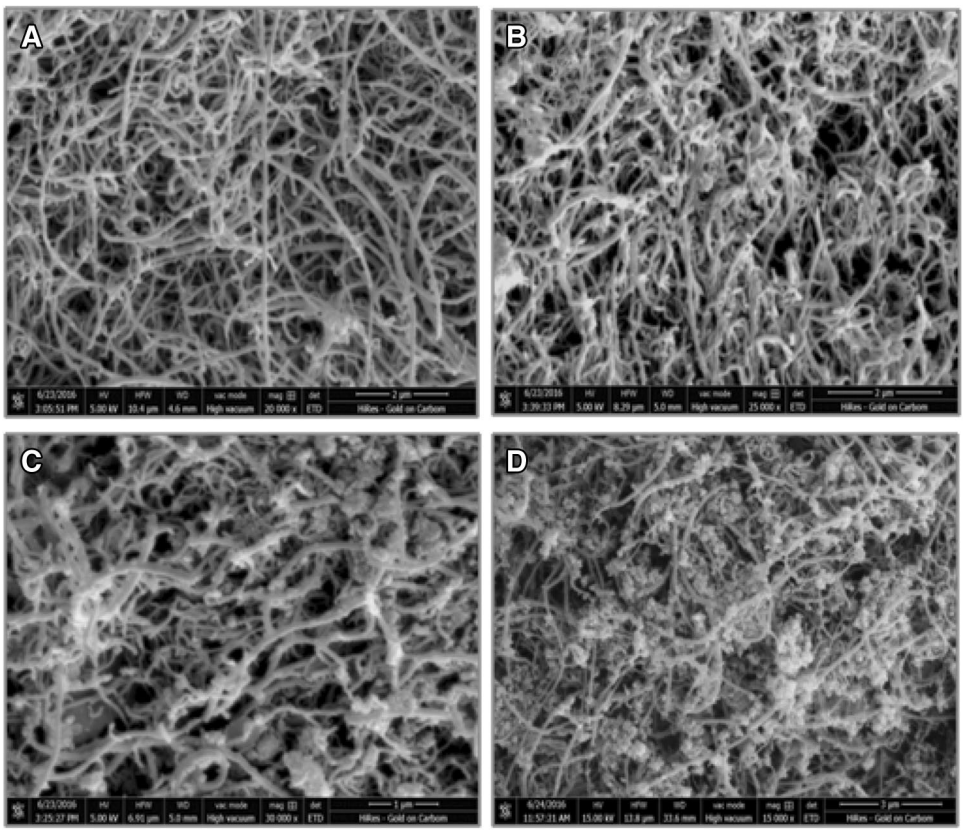

Fig. 2 FESEM micrographs of **a** MWCNT, **b** MWCNT/Cu NP, **c** Ag NP/MWCNT and **d** Ag NP/MWCNT/Cu NP

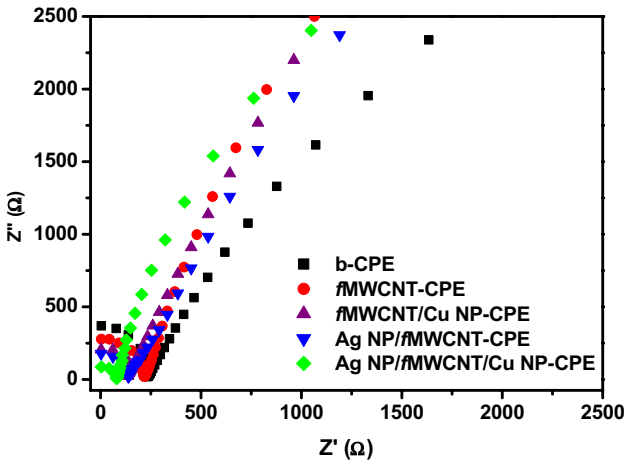

Fig. 3 Nyquist plot of 1.0 mM $Fe(CN)_6^{3-/4-}$ in 0.1 M KCl at different electrodes

plot for 1.0 mM $Fe(CN)_6^{3-/4-}$ in 0.1 M KCl showed a significant difference in responses of electrodes as shown in Fig. 3. The semicircle elements observed at high frequency region (10^{-1}–10^6 Hz) corresponds to the charge transfer limiting process and charge transfer resistance (R_{ct}).

3.4 Electrocatalytic voltammetric behavior of ADB

The electrocatalytic behavior of the designed electrochemical sensors towards the voltammetric determination of 4.5×10^{-7} M Amlodipine in 0.05 M BR buffer (pH 10.5 ± 0.01) at bare and modified CPEs were observed by using CV and adsorptive square wave voltammetry (AdSWV). Cyclic voltammograms of ADB exhibited a single well defined, irreversible, anodic peak in the potential range from 0.0 mV to $+8.0 \times 10^2$ mV. The anodic peak observed at 5.2×10^2 mV is attributed to the oxidation of Amlodipine moiety which was not accompanied by any cathodic peak on reversing the direction of scan, indicating the irreversible nature of reduction process. Figure 4A and B compares the electrocatalytic property of bare and modified CPEs towards the determination of 4.5×10^{-7} M ADB.

3.5 Optimization of conditions

AdSWV was employed to optimize parameters that affect the sensitivity and propose an accurate and precise determination of ADB in pharmaceutical and biological samples. A variety of buffers with varying strengths were used in determining amlodipine in test solutions. The best results in terms of peak current and voltammogram

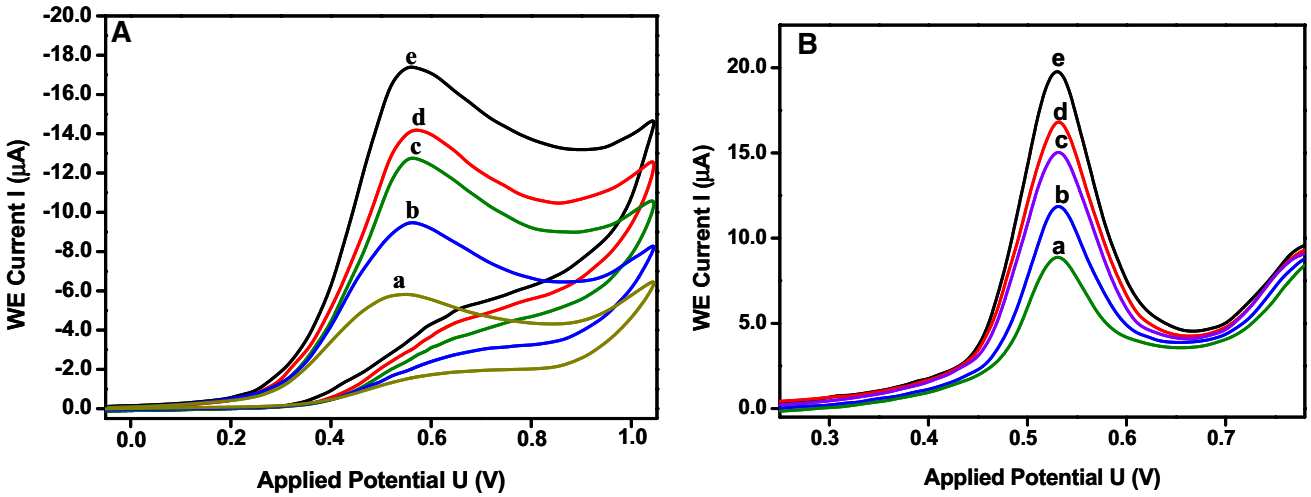

Fig. 4 **A** Cyclic and **B** adsorptive square wave voltammograms of 4.5×10^{-7} M amlodipine in 0.05 M BR buffer (pH 10.5) at (a) bare CPE, (b) *f*MWCNT-CPE, (c) *f*MWCNT/Cu NP-CPE (d) Ag NP/*f*MWCNT-CPE and (e) Ag NP/*f*MWCNT/Cu NP-CPE

shape were obtained with 0.05 M BR buffer of pH 10.5. A linear plot was observed with a slope of 56.2 mVpH^{-1} when solution pH was plotted against peak potential. The slope value is close to Nernst's value of 59 mV pH^{-1} defining that equal electrons and protons are participating in electrode process.

The stripping peak currents was further increased by varying the deposition potential and time from -5.0×10^{2} mV to $+5.0\times10^{2}$ mV and 0–150 s respectively. Best peak current was observed when setting a deposition potential of -5.0×10^{2} mV for 120 s of accumulation time. Further the instrumental parameters like square wave frequency, step potential of staircase waveform and pulse amplitude were optimized for better peak resolutions. An increase in peak current was observed with increasing frequency however peak crest broadened at higher frequencies. Hence, for sharper peak 40 Hz frequency was found optimum. The increased step potential and pulse amplitudes tend to increase both peak current and background current. Thus to have better peak current and sharper peak, 10 mV step potential and 20 mV pulse amplitude was optimized resulting in enhanced sensitivity.

3.6 Kinetic parameters of electrocatalytic oxidation

3.6.1 Cyclic voltammetric study

The cyclic voltammograms of 4.5×10^{-7} M amlodipine in scan range from 10–200 mVs^{-1} were recorded in 0.05 M BR buffer (pH = 10.5) at Ag NP/*f*MWCNT/Cu NP-CPE and was employed for the determination of various electrokinetic parameters. The relation between the peak current and peak potential with scan rate illustrates whether the electrode process is diffusion or adsorption controlled. The peak current increases gradually with increasing scan rate, while the peak potential shifted anodically indicating the oxidation of amlodipine is an irreversible process (Fig. 5). The plot of log I_p vs log υ, (Fig. 5 inset) exhibited a linear relationship expressed by following equation:

$$\log I_p(\mu A) = 0.942 \log \nu + 14.439 \quad R^2 = 0.997 \tag{2}$$

The value of slope, 0.942 is near to theoretical value of 1.0 for a typical surface adsorptive species. This finding was

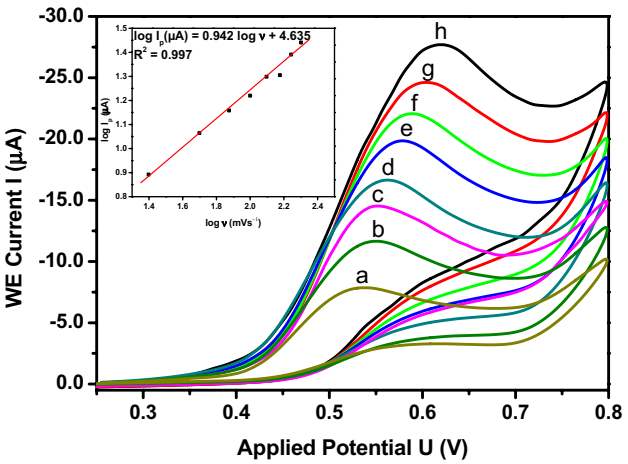

Fig. 5 Cyclic voltammograms of 4.5×10^{-7} M amlodipine in BR buffer (pH 10.5) at Ag NP/*f*MWCNT/Cu NP-CPE with a scan rate of (a) 25 mVs^{-1}, (b) 50 mVs^{-1}, (c) 75 mVs^{-1}, (d) 100 mVs^{-1}, (e) 125 mVs^{-1}, (f) 150 mVs^{-1}, (g) 175 mVs^{-1} and (h) 200 mVs^{-1}. Inset is plot of logarithm of peak current *vs.* logarithm of scan rate

well supported by obtaining linear Randles-Sevick plot (I_p vs υ). For an irreversible electrode process, n (number of electrons transferred), α (electron transfer coefficient), E^0 (formal redox potential) and k^0 (standard heterogeneous rate constant of the reaction) can be calculated from Laviron's equation [32].

$$E_p = E^0 + \left(\frac{2.303RT}{\alpha nF}\right)\log\frac{RTK^0}{\alpha nF} + \left(\frac{2.303RT}{\alpha nF}\right)\log v \quad (3)$$

$$W_{1/2} = \frac{2.44RT}{\alpha nF} = \frac{0.0626}{\alpha n}(298K) \quad (4)$$

where, $W_{1/2}$ is the half width of peak, υ is the scan rate and R, T and F are molar gas constant, temperature and Faraday's constant respectively. The value of αn can be evaluated from the slope of E_p *vs* log υ, the slope was found to be 0.083 and by substituting the values of R and F and taking T = 298 K, αn was calculated to be 0.526. According to Bard and Faulkner [31], α can be given as:

$$\alpha = \frac{47.7}{E_p - E_{p/2}} \quad \text{mV at 298 K} \quad (5)$$

where, E_p is peak potential and $E_{p/2}$ is the half peak potential where current is half of the peak value. Thus, α was calculated to be 0.254 and from this number of electron transferred (n) in the electro-oxidation of amlodipine was calculated as 2.07 (~2 electron process).

3.6.2 Controlled potential coulometric behavior and plausible electrode reaction mechanism

Cyclic and adsorptive stripping square wave voltammetric studies have shown that amlodipine undergoes electrochemical oxidation in BR buffer at pH 10.5. The electrode process is irreversible at the modified CPEs and pH studies confirmed the involvement of equal number of protons and electrons. By using controlled potential coulometry, the number of electrons transferred (n) can be estimated from the charge consumed by the electrolysis of desired concentration of amlodipine. For this 25 nM, 50 nM and 75 nM solution of amlodipine was placed in voltammetric cell and electrolysis was carried out at $+4.0\times10^2$ mV against Ag/AgCl reference electrode. During the electrolysis, solutions were continuously stirred and purged with nitrogen. Number of electrons 'n' transferred was calculated using the equation Q = nFN, were Q is charge in coulombs, F is Faraday's constant and N is number of moles of the substance. Three replicate experiments were performed and the value of 'n' was found to be 1.93, 2.04 and 1.97, thus indicating that the electrode reaction is a two electron process as shown in Scheme 2.

The saturated adsorption capacities of the electrodes were evaluated from chronocoulometric experiment. Faradic charge due to oxidation (Q_{ads}) of amlodipine is determined from Q vs $t^{1/2}$ curves using Anson equation [33]:

$$Q = \frac{2nFAc(Dt)^{\frac{1}{2}}}{\pi^{\frac{1}{2}}} + Q_{dl} + Q_{ads} \quad (8)$$

where Q_{dl} is the double-layer charge and D is diffusion coefficient. Q_{dl} is supposed to remain similar in absence and presence of amlodipine. The Q-t curves are obtained by applying potential of $+4.0\times10^2$ mV in the absence and presence of 4.5×10^{-7} M amlodipine at electrode surface (Fig. 6). Plot of Q vs $t^{1/2}$ were drawn after extracting data from Q-t curves and displayed in Fig. 6 inset. The plots of Q vs $t^{1/2}$ showed parallel and linear relationships in absence and presence of amlodipine and the value of Q_{ads} is estimated from the intercepts and tabulated in Table 1. The experiment is recorded with all modified and bare CPEs. The surface coverage ((Γ*) for all electrodes is estimated using the equation [34]:

$$Q_{ads} = nFA\Gamma^* \quad (9)$$

Scheme 2 The possible oxidation mechanism of ADB

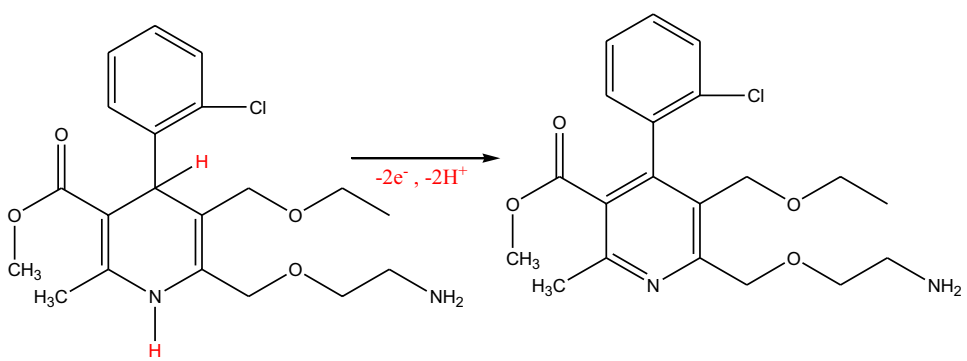

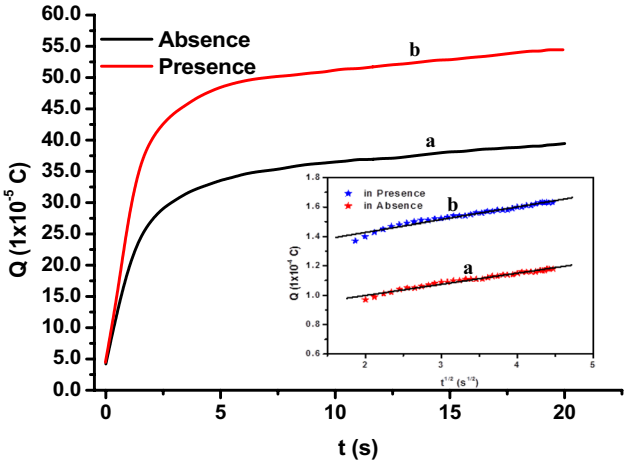

Fig. 6 Chronocoulometric response curves obtained in (a) absence and (b) presence of 4.5×10^{-7} M amlodipine in BR buffer (pH = 10.5) at the Ag NP/*f*MWCNT/Cu NP-CPE. **Inset:** The dependency of charge Q (10^{-5}) *vs.* $t^{1/2}$ data derived from chronocoulometric curves (a) absence and (b) presence of 4.5×10^{-7} M amlodipine

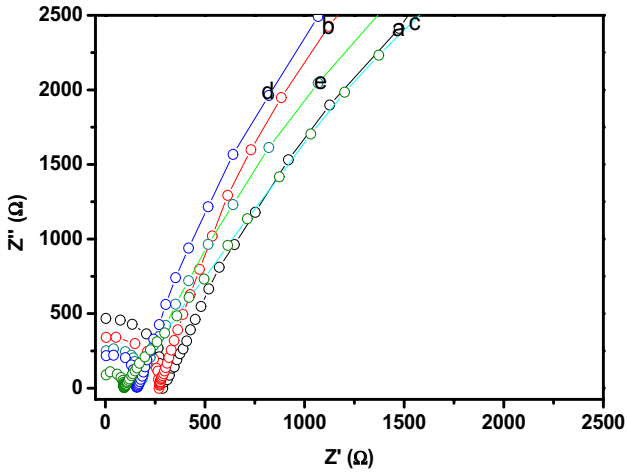

Fig. 7 Nyquist plot observed in presence of 4.5×10^{-7} M amlodipine at (a) b-CPE (b) *f*MWCNT-CPE (c) *f*MWCNT/Cu NP-CPE (d) Ag NP/ *f*MWCNT-CPE (e) Ag NP/*f*MWCNT/Cu NP-CPE

Table 1 Surface coverage (Γ^*) and charge due to adsorption (Q_{ads}) of electrochemical reaction at electrode surface:

Electrode	Q_{ads} (1×10^{-4} C)	Γ^* (10^{-10} mol cm^{-2})
b-CPE	0.0142	1.42
*f*MWCNT-CPE	0.204	3.88
*f*MWCNT/Cu NP-CPE	0.702	6.98
Ag NP/*f*MWCNT-CPE	1.110	9.05
AgNP/*f*MWCNT/Cu NP-CPE	2.306	12.33

Table 2 Charge transfer resistance (R_{ct}) and apparent electron transfer rate constant (k_{app}) of bare and modified electrodes in 4.5×10^{-7} M amlodipine

Electrode	R_{ct} (Ω)	k_{app} ($\times10^{-5}$ cm s^{-1})
b-CPE	497	1.19
*f*MWCNT-CPE	326	1.44
*f*MWCNT/Cu NP-CPE	205	2.52
Ag NP/*f*MWCNT-CPE	174	3.44
Ag NP/*f*MWCNT/Cu NP-CPE	83	9.39

3.6.3 Impedance study

Electrochemical impedance spectroscopy (EIS) is an excellent technique to elucidate properties like charge transfer resistance (R_{ct}), apparent electron transfer rate constant (k_{app}), double layer capacitance and electro-catalytic oxidation or reduction process at the electrode-analyte interface [16]. The electrode having lower R_{ct} value and higher k_{app} is more favorable for redox reactions. EIS study of 4.5×10^{-7} M amlodipine at the surface of bare and all modified CPEs was carried out to assess their R_{ct} and k_{app}. Figure 7 represents the Nyquist plot of 4.5×10^{-7} M amlodipine on bare and modified CPEs. The lower diameter of semi-circle domains obtained in the Nyquist plots upon modification results in decreased R_{ct} value, thus providing faster electron transfer for oxidation of amlodipine at the electrode surface. The R_{ct} value obtained for Ag NP/*f*MWCNT/Cu NP-CPE is much smaller than other designed electrodes. The values obtained are 63 Ω, 172 Ω, 235 Ω, 412 Ω and 496 Ω for Ag NP/*f*MWCNT/Cu NP-CPE, Ag NP/*f*MWCNT-CPE, *f*MWCNT/Cu NP-CPE, fMWCNT-CPE and CPE respectively. The apparent electron transfer rate constant (k_{app}) is calculated using equation [35]:

$$k_{app} = \frac{RT}{F^2 R_{ct} C} \quad (10)$$

where R_{ct} is the resistance to charge transfer, C is the concentration of ADB and other terms have their usual meaning. The calculated values of k_{app} for different electrodes are listed in Table 2. The results confirm faster electrons transfer at Ag NP/*f*MWCNT/Cu NP-CPE relative to the other electrodes which is due to combinatorial excellent electric properties of silver and copper.

3.7 Analytical applications

3.7.1 Linearity and calibration graph

The analytical performance of the proposed method as an analytical tool was validated by measuring peak current (I_p) as a function of concentration of amlodipine by AdSWV

at Ag NP/*f*MWCNT/Cu NP-CPE. The calibration plot of I_p versus concentration gives best linear correlation in the concentration range of 2.0×10^{-8} M to 6.3×10^{-6} M using AdSWV in BR buffer (pH 10.5) at Ag NP/*f*MWCNT/Cu NP-CPE. The limit of detection (LOD) and limit of quantification (LOQ) were calculated using $LOD = \frac{3s}{m}$ and $LOQ = \frac{10s}{m}$ equations [3]. Where *s* is the standard deviation of the intercept (n = 5), m is the slope of the regression line. The calculated LOD was found to be 5.16×10^{-10} M with LOQ was amounted to be 1.72×10^{-9} M. The %RSD for five measurements at each concentration (n = 5) were ranged from 1.21% to 2.17%. Table 3 compares the response characteristics of proposed method with some other reported analytical methods for the determination of ADB.

3.7.2 Accuracy and precision

The accuracy and precision of the proposed method at the fabricated Ag NP/*f*MWCNT Cu NP-CPE was validated by spiking with known amounts (pre-analyzed) of test solution under optimized condition. The accuracy (% bias) was expressed in terms of mean relative error. The % bias values varies between – 0.4% to 0.05% which are highly acceptable and show better accuracy of the method. The precision of the proposed method was determined by analyzing amlodipine in pre-analyzed sample solutions for four successive days with five replications. The % recovery and % RSD (relative standard deviation) based on the average of five replicates were determined. The results confirm better accuracy and precision with low mean variation coefficient of 0.119% and mean % recoveries of 100.01 for AdSWV.

3.7.3 Stability and reproducibility

To study the fabrication reproducibility of Ag NP/*f*MWCNT/Cu NP-CPE, five electrodes were designed via same procedure and applied for analyzing 4.5×10^{-7} M amlodipine under optimized parameters with AdSWV. The average % RSD of peak current and peak potential for average of 5 replicated analyses on each fabricated electrode are 1.027% and 0.185% respectively. The repeatability of developed method over single modified electrode was estimated by analyzing 10 replicate determination of 4.5×10^{-7} M test solution using AdSWV. The mean concentration was found to be 4.997×10^{-7} M with a standard deviation of 0.0036 and % RSD of 1.014. The results revealed that modified electrode has high reproducibility and repeatability in both fabrication procedure and signal determination.

For long term stability of Ag NP/*f*MWCNT/Cu NP-CPE the electrode was stored at room temperature for 10 to 25 days. The voltammograms were recorded for 4.5×10^{-7} M amlodipine and compared with the voltammogram recorded with freshly prepared electrode for same concentration. The result (for n = 5) reveal that peak current deflected a tad (± 2.19% of initial current) with % RSD of 1.027 which indicates the good stability of electrode. These results established good stability and capability of modified electrode to perform repeated measurements (Fig. 8).

3.7.4 Analysis of real samples

The feasibility of Ag NP/*f*MWCNT/Cu NP-CPE and of the developed procedure was verified by analyzing amlodipine in real samples (Human blood plasma, serum and urine and pharmaceutical formulations) under optimized condition. Initially, no voltammetric response corresponding to amlodipine was observed indicating that real sample was either absolutely free of amlodipine or may have concentration below detection limit. The quantitative determination of spiked amlodipine was carried out by standard addition method and calibration curve were drawn to obtain the recovery result. The biological samples spiked with three different known concentrations of amlodipine and voltammograms were recorded using AdSWV. The results are summarized in Table 4**.** The % recoveries indicated the sensitivity of modified electrode and applicability of the proposed method in real samples.

Table 3 Comparison of various reported analytical methods for the determination of amlodipine:

Analytical method	Linear range	LOD	References
Adsorptive square-wave anodic stripping voltammetry	4.0×10^{-8} M to 2.0×10^{-6} M	1.4×10^{-8} M	[19]
Differential pulse stripping voltammetry	1.0×10^{-8} M to 3.0×10^{-7} M	5.0×10^{-9} M	[21]
Square wave voltammetry	5.0×10^{-9} M to 1.0×10^{-6} M	1.0×10^{-9} M	[36]
Spectrofluorometric method	2.0×10^{-7} M to 3.6×10^{-6} M	2.5×10^{-8} M	[37]
Adsorptive square wave voltammetry	2.0×10^{-8} M to 6.3×10^{-6}	5.16×10^{-10} M	Present work

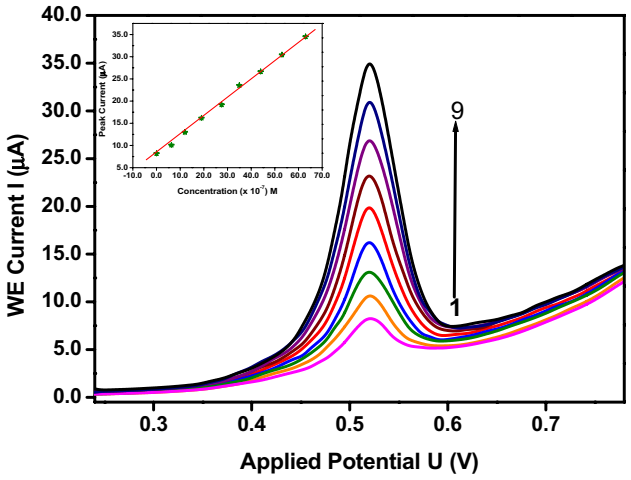

Fig. 8 Adsorptive square wave voltammograms of (1 → 9) 0.002 μM, 0.630 μM, 1.20 μM, 1.90 μM, 2.75 μM, 3.50 μM, 4.40 μM, 5.30 μM and 6.30 μM amlodipine in BR buffer (pH = 10.5) at Ag NP/*f*MWCNT/Cu NP-CPE surface. Inset: Linear dependence of peak current with concentration of amlodipine

Table 4 Determination of amlodipine in real samples using AdSWV

Sample	Spiked amount	Found	Recovery %	RSD %
Amlodac	5 mg (label claim)	4.989	99.78	1.12
Amlopin	5 mg (label claim)	4.998	99.96	0.19
Serum	0.8 μM	0.801 μM	100.12	1.13
	0.6 μM	0.599 μM	99.83	2.07
	0.4 μM	0.403 μM	100.75	0.94
Plasma	0.8 μM	0.798 μM	99.75	1.26
	0.6 μM	0.594 μM	99.00	1.84
	0.4 μM	0.396 μM	99.00	1.05
Urine	0.8 μM	0.802 μM	100.25	0.84
	0.6 μM	0.601 μM	100.16	0.91
	0.4 μM	0.398 μM	99.50	1.17

4 Discussion

Our results confirm that the successful development of highly sensitive, selective and stable Ag NP/**f**MWCNT/Cu NP-CPE and its efficient response towards the calcium channel blocker drug amlodipine besylate in blood plasma and various pharmaceutical preparations with a low detection limit of 5.16×10^{-10} M. The observed ΔE_p values for *f*MWCNT-CPE, *f*MWCNT/Cu NP-CPE, Ag NP/*f*MWCNT-CPE and Ag NP/*f*MWCNT/Cu NP-CPE are 2.41×10^2 mV, 1.95×10^2 mV, 1.44×10^2 mV and 87 mV respectively, confirmed the improvisation in the performance towards the detection of ADB drug which might be attributed to the successful deposition of Ag NPs and Cu NPs on the *f*MWCNT-CPE**.** The EIS results implies that the charge transfer resistance (R_{ct}) at Ag NP/*f*MWCNT/Cu NP-CPE ($R_{ct} = 67.4\ \Omega$) is lower than that of AgNP/*f*MWCNT-CPE ($R_{ct} = 147\ \Omega$), *f*MWCNT/CU NP-CPE ($R_{ct} = 185\ \Omega$), *f*MWCNT-CPE ($R_{ct} = 324\ \Omega$) and b-CPE ($R_{ct} = 415\ \Omega$). These observations indicate excellent combined electrocatalytic property of Ag NPs, Cu NPs and *f*MWCNT in addition to properties like high aspect ratio, good conductivity, easier and faster charge transfer at electrode surface**.** The increased electron transfer rate, high electroactive surface area and admirable electrode conductivity of nanoparticles was evident by observing increased peak current intensities at the modified electrodes. The Ag NP film over fMWCNT/Cu NP hybrid exerts a significant catalytic activity in the oxidation of ADB (Fig. 4A, B).

5 Conclusion

AgNPs were successfully deposited on *f*MWCNT/Cu NP-CPE via electrocatalytic process. The designed electrode (AgNPs/**f**MWCNT/Cu NP-CPE) exhibits excellent structural features like large electroactive surface area, faster electron transfer rates, predominant electrocatalytic activity, acceptable reproducibility (both in fabrication procedure and signal determination) and long-term stability. The sensor evinced high efficacy towards the determination of a hyper-tensive drug ADB. Furthermore, the sensor demonstrated a linear response for ADB in the range 2.0×10^{-8} M to 6.3×10^{-6} M and with a low detection limit of 5.16×10^{-10} M. In addition, this study can open the way for designing cheap and highly efficient sensors for the analysis of forensic drugs, quality control processes, heavy metal analysis, water quality analysis as well as future potential applications in this filed.

Acknowledgements Authors are highly thankful to the Department of Chemistry and Sophisticated Instrumentation Laboratory (SIL) of Dr. Hari Singh Gour University, Sagar, India for providing the necessary facilities to complete the work.

Author contributions First and second author has contributed 50% and rest of the contribution from other authors.

Data availability All data is given in the manuscript.

Compliance with ethical standards

Competing interests The authors declare that they have no competing interests.

References

1. Kulkarni DR, Malode SJ, Prabhu KK, Ayachit NH, Kulkarni RM, Shetti NP (2020) Development of a novel nanosensor using Ca-doped ZnO for antihistamine drug. Mater Chem Phys 246:122791
2. Dakshayinia BS, Reddy KR, Mishrac A, Shetti NP, Maloded SJ, Basuc S, Naveene S, Raghue AV (2019) Role of conducting polymer and metal oxide based hybrids for application in ampereometric sensors and biosensors. Microchem J 147:7–24
3. Shetti NP, Malode SJ, Bukkitgar SD, Bagihalli GB, Kulkarni RM, Pujari SB, Reddy KR (2019) Electro-oxidation and determination of nimesulide at nanosilica modified sensor. Mater Sci Energy Technol 2:396–400
4. Shetti NP, Shanbhaga MM, Malode SJ, Srivastava RK, Reddy KR (2020) Amberlite XAD-4 modified electrodes for highly sensitive electrochemical determination of nimesulide in human urine. Microchem J 153:104389
5. Bukkitgar SD, Shetti NP, Malladi RS, Reddy KR, Kalanur SS, Aminabhavi TM (2019) Novel ruthenium doped TiO2/reduced graphene oxide hybrid as highly selective sensor for the determination of ambroxol. J Mol Liq 300:112368
6. Shetti NP, Malode SJ, Nayak DS, Bukkitgar SD, Bagihalli GB, Kulkarni RM, Reddy KR (2020) Novel nanoclay-based electrochemical sensor for highly efficient electrochemical sensing nimesulide. J Phys Chem Solids 137:109210
7. Honakeri NC, Malode SJ, Kulkarni RM, Shetti NP (2020) Electrochemical behavior of diclofenac sodium at coreshell nanostructure modified electrode and its analysis in human urine and pharmaceutical samples. Sensors Int 1:100002
8. Bhakta AK, Kumari S, Hussain S, Martis P, Mascarenhas RJ, Delhalle J, Mekhalif Z (2019) Synthesis and characterization of maghemite nanocrystals decorated multi-wall carbon nanotubes for methylene blue dye removal. J Mater Sci 54:200–216
9. Manasa G, Mascarenhas RJ, Satpati AK, Basavaraja BM, Kumar S (2018) An electrochemical Bisphenol F sensor based on ZnO/G nano composite and CTAB surface modified carbon paste electrode architecture. Colloids Surf B 170:144–151
10. Veera Y, Reddy M, Sravani B, Maseed H, Łuczak T, Osińska M, Sarma LS, Srikanth VVSS, Madhavi G (2018) Ultrafine Pt-Ni bimetallic nanoparticles anchored on reduced graphene oxide nanocomposites for boosting electrochemical detection of dopamine in biological samples. New J Chem 42:16891–16901
11. Sravani B, Raghavendra P, Chandrasekhar Y, Veera Y, Reddy M, Sivasubramanian R, Venkateswarlu K, Madhavi G, Subramanyam SL (2020) Immobilization of platinum-cobalt and platinum-nickel bimetallic nanoparticles on pomegranate peel extract-treated reduced graphene oxide as electrocatalysts for oxygen reduction reaction. Int J Hydrogen Energ 45:7680–7690
12. Chen A, Chatterjee S (2013) Nanomaterials based electrochemical sensors for biomedical applications. Chem Soc Rev 42:5425–5438
13. Brahman PK, Suresh L, Lokesh V, Nizamuddin S (2016) Fabrication of highly sensitive and selective nanocomposite film based on CuNPs/Fullerene-C_{60}/MWCNTs: an electrochemical nanosensor for trace recognition of paracetamol. Anal Chim Acta 917:107–116
14. Ren J, Li L, Cui M, Zhai M, Yu C, Ji X (2016) Nitrobenzene electrochemical sensor based on silver nanoparticle supported on poly-melamine functional multi-walled carbon nanotubes. Ionics 22:1937–1947
15. Habibi B, Jahanbakhshi M (2014) Silver nanoparticles/multi walled carbon nanotubes nanocomposite modified electrode: Voltammetric determination of clonazepam. Electrochim Acta 118:10–17
16. Zargar B, Parham H, Hatamie A (2014) Electrochemical investigation and stripping voltammetric determination of captopril at CuO nanoparticles/multi-wall carbon nanotube nanocomposite electrode in tablet and urine samples. Anal Methods 7:1026–1035
17. Carvalho M, Oliveria CH, Mendes GD, Sucupira M, Moraces ME, De NG (2002) Amlodipine bioequivalence study: quantifiqation by LC coupled to tandem mass spectrometry. Biopharm Drug Dispos 22:383–390
18. Bhatt J, Singh S, Shah SGB, Kambli S, Ameta SA (2007) Rapid and sensitive LC-MS/MS method for estimation of Amlodipine in human plasma. Biomed Chromatogr 21:169–175
19. Gazy AA (2004) Determination of Amlodipine Besylate by adsorptive square-wave anodic stripping Voltammetry on glassy carbon electrode in tablets and biological fluids. Talanta 62:575–582
20. Sridhar K, Sastry CSP, Reddy MN, Sankar DG, Srinivas KR (1997) Spectrophotometric determination of Amlodipine Besylate in pure forms and Tablets. Anal Lett 30:121–133
21. Sikkander ARM, Vedhi C, Manisankar P (2012) Electrochemical determination of calcium channel blocker drugs using multiwall carbon nanotube-modified glassy carbon electrode. Int J Ind Chem 3:29–36
22. Sikkander ARM, Vedhi C, Manisankar P (2011) Electrochemical stripping studies of Amlodipine using MWCNT modified Glassy carbon electrode. Chem Mater Res 1:1–7
23. Burguete CP, Linares-Solano A, Rodríguez-Reinoso F, Lecea CSM (1989) The effect of oxygen surface groups of the support on platinum dispersion in Pt/carbon catalysts. J Catal 115:98–106
24. Cuentas-Gallegos AK, Martínez-Rosales R, Rincón ME, Hirata GA, Orozco G (2006) Design of hybrid materials based on carbon nanotubes and polyoxometalates. Opt Mater 29:126–133
25. Smith B, Wepasnick K, Schrote KE, Cho HH, Ball WP, Fairbrother DH (2009) Influence of surface oxides on the colloidal stability of multi-walled carbon nanotubes: a structure–property relationship. Langmuir 25:9767–9776
26. Avilés F, Cauich-Rodríguez JV, Moo-Tah L, May-Pat A, Vargas-Coronado R (2009) Evaluation of mild acid oxidation treatments for MWCNT functionalization. Carbon 47:2970–2975
27. Haydar S et al (2000) Regularities in the temperature-programmed desorption spectra of CO2 and CO from activated carbons. Carbon 38:1297–1308
28. Wilson H et al (2016) Electrical monitoring of sp3 defect formation in individual carbon nanotubes. J Phy Chem C 120:1971–1976
29. Gao C, Li W, Jin YZ, Kong H (2006) Facile and large-scale synthesis and characterization of carbon nanotube/silver nanocrystal nanohybrids. Nanotechnology 17:2882–2890
30. Habibi B, Jahanbakhshi M (2006) Silver nanoparticles/multi walled carbon nanotubes nanocomposite modified electrode: Voltammetric determination of clonazepam. Electrochim Acta 118:10–17
31. Pandit UJ, Khan I, Wankar S, Raj KK (2015) Limaye SN (2015) Development of an electrochemical method for the determination of bicalutamide at the SWCNT/CPE in pharmaceutical preparations and human biological fluids. Anal Methods 7:10192–10198
32. Qiao W, Wang L, Ye B, Li G, Li J (2015) Electrochemical behavior of palmatine and its sensitive determination based on an electrochemically reduced L-methionine functionalized graphene oxide modified electrode. Analyst 140:7974–7983
33. Anson F (1964) Application of potentiostatic current integration to the study of the adsorption of cobalt (III)–(ethylenedinitrilotetraacetate)) on mercury electrodes. Anal Chem 36:932–934
34. Qiao W, Wang L, Ye B, Li G, Li J (2015) Electrochemical behaviour of palmatine and its sensitive determination based on an

electrochemically reduced L-methionine functionalized graphene oxide modified electrode. Analyst 140:7974–7983
35. Maringa A, Mugadza T, Antunes E, Nyokong T (2013) Characterization and electrocatalytic behaviour of glassy carbon electrode modified with nickel nanoparticles towards amitrole detection. J Electroanal Chem 700:86–92
36. Goyal RN, Bishnoi S (2010) Voltammetric determination of amlodipine besylate in human urine and pharmaceuticals. Bioelectrochemistry 79:234–240
37. Shaalan RA, Belal TS (2010) Simultaneous Spectrofluorimetric determination of amlodipine besylate and valsartan in their combined tablets. Drug Test Anal 2:489–493